Running head: Cyanide action in root hair elongation

Corresponding author: Dr. I. García. Instituto de Bioquímica Vegetal y Fotosíntesis. Consejo Superior de Investigaciones Científicas and Universidad de Sevilla. Avenida Américo Vespucio, 49, 41092 Sevilla, Spain. Tel: + 34 954 489 500. Fax: +34 954 460 165. Email: irene.garcia@ibvf.csic.es

Subject area: growth and development

This manuscript contains 4 black and white figures, 3 color figures, 2 tables, 7 supplementary figures and 1 supplementary video.

ß-Cyanoalanine synthase action in root hair elongation is exerted at early steps of the root hair elongation pathway and is independent on direct cyanide inactivation of NADPH oxidase

Running head: Cyanide action in root hair elongation

Lucía Arenas-Alfonseca, Cecilia Gotor, Luis C. Romero and Irene García*

Instituto de Bioquímica Vegetal y Fotosíntesis, Consejo Superior de Investigaciones Científicas and Universidad de Sevilla, Avenida Américo Vespucio, 49, 41092 Sevilla, Spain

* Email: irene.garcia@ibvf.csic.es. Fax: +34 954 460 165

Abbreviations

ACC: 1-aminocyclopropane-1-carboxylic acid

bHLH: basic helix-loop-helix

CAS: ß-cyanoalanine synthase

COB: 2-hydroxocobalamin

CT: cycle threshold

FW: fresh weight

GFP: green fluorescent protein

H_2DCFDA: 2',7'-dichlorodihydrofluorescein diacetate

NBT: nitro blue tetrazolium

ORF: open reading frame

ROS: reactive oxygen species

TF: transcription factor

XTT: 3′-[1-[(phenylamino)-carbony]-3,4-tetrazolium]-bis(4-methoxy-6-nitro)benzene-sulfonic acid

Abstract

In *Arabidopsis thaliana*, cyanide is produced concomitantly with ethylene biosynthesis and is mainly detoxified by the ß-cyanoalanine synthase CAS-C1. In roots, CAS-C1 activity is essential to maintain a low level of cyanide for proper root hair development. Root hair elongation relies on polarized cell expansion at the growing tip, and we have observed that CAS-C1 locates in mitochondria and accumulates in root hair tips during root hair elongation, as shown by observing the fluorescence in plants transformed with the translational construct *ProC1:CASC1-GFP*, containing the complete *CAS-C1* gene fused to *GFP*. Mutants in the *SUPERCENTIPEDE* (*SCN1*) gene, that regulate the NADPH oxidase *RHD2*/*AtrbohC,* are affected at the very early steps of the development of root hair that do not elongate and do not show a preferential localization of the GFP accumulation in the tips of the root hair primordia. Root hairs of mutants in *CAS-C1* or *RHD2*/*AtrbohC,* which catalyzes the generation of ROS and the Ca^{2+} gradient*,* correctly start to grow out but they do not elongate either. Genetic crosses between the *cas-c1* mutant and *scn1* or *rhd2* mutants were performed and the detail phenotypic and molecular characterization of the double mutants demonstrate that *scn1* mutation is epistatic to *cas-c1* and *cas-c1* is epistatic to *rhd2* mutation, indicating that CAS-C1 acts in early steps of the root hair development process. Moreover, our results show that the role of CAS-C1 in root hair elongation is independent of H_2O_2 production and of a direct NADPH oxidase inhibition by cyanide.

Keywords

Arabidopsis thaliana, ß-Cyanoalanine Synthase, Root Hair, Cyanide, SCN1, RHD2.

Introduction

Cyanide is extensively present in all organisms, including bacteria, fungi, insects and plants. However, cyanide is a toxic compound due to its high reactivity with keto compounds and Schiff bases and because it chelates di- and trivalent metal ions in the prosthetic groups of metalloproteins (Donato et al. 2007). Mitochondria is the major target of cyanide, where it binds to the heme iron of cytochrome c oxidase, blocking the respiratory chain (Cooper and Brown 2008). In non-cyanogenic plant species such as *A. thaliana*, the main source of cyanide is the biosynthesis of the hormone ethylene, which is involved in regulating numerous developmental processes and responses to stress conditions (Bleecker and Kende 2000), and the biosynthesis of the phytoalexin camalexin, which is formed when *A. thaliana* plants are infected by a large variety of microorganisms (Glawischnig 2007). Therefore, under certain developmental or environmental conditions, plants produce significant amounts of cyanide that may be harmful to their cells, requiring detoxification. To keep cyanide below toxic concentrations, plants possess different metabolic pathways, the main pathway of which is that involving ß-cyanoalanine synthase (CAS) ((Machingura et al. 2016) and references therein).

Arabidopsis plants express the mitochondrial ß-cyanoalanine synthase CAS-C1 (formerly CYS-C1, (Romero et al. 2014) (Watanabe et al. 2008)), which, together with the O-acetylserine(thiol)lyases (OASTLs), belongs to the family of ß-substituted alanine synthase enzymes. CAS is a pyridoxal phosphate-dependent enzyme that uses cysteine to detoxify cyanide by converting cyanide and cysteine in hydrogen sulfide (H_2S) and ß-cyanoalanine. H_2S also blocks the mitochondrial respiratory pathway and therefore needs to be detoxified by the true OASTL OAS-C, which incorporates H_2S to O-acetylserine (OAS) to produce cysteine, which is recycled by CAS-C1 to detoxify cyanide, thus completing the cyanide detoxification cycle in mitochondria (Alvarez et al. 2012). ß-Cyanoalanine is converted to Asn, Asp and ammonia by NIT4 class nitrilases, thereby recycling the nitrogen for plant utilization (Piotrowski 2008).

Cyanide at non-toxic levels has been suggested to perform regulatory roles in different physiological processes. In animal systems, for example, it has been hypothesized to act as a neuromodulator (Cipollone and Visca 2007). In plants, exogenously applied cyanide can act as a regulator of seed dormancy and germination (Bethke et al. 2006; Chivasa and Carr 1998; Cohn and Hughes 1986; Seo et al. 2011; Siegien and Bogatek 2006; Wong et al. 2002) and play a role in resistance to viral and fungal pathogens (Bethke et al. 2006; Chivasa and Carr 1998; Cohn and Hughes 1986; Seo et al. 2011; Siegien and Bogatek 2006; Wong et al. 2002). Our previous investigation on the *CAS-C1* null mutant has provided insight into the role of the endogenously produced

cyanide in Arabidopsis. Loss-of-function mutation of the *CAS-C1* gene leads to a non-toxic increase in cyanide (Garcia et al. 2010) and an altered immune response, i.e., increased susceptibility to the necrotrophic fungus *Botrytis cinerea* and increased tolerance to the biotrophic pathogens *Pseudomonas syringae* pv. *tomato DC3000* and beet curly top virus (Garcia et al. 2013). Because the null mutant exhibits an induced alternative oxidase respiration, reactive oxygen species (ROS) accumulation and salicylic acid-dependent pathway induction, it was hypothesized that cyanide might generate a mitochondrial signal, unknown to date, that could modulate the plant immune system (Garcia et al. 2014). The *cas-c1* mutant also exhibits a root hairless phenotype, which is reverted either genetically by complementation with the corresponding *CAS-C1* gene or chemically by the addition of the cyanide antidote hydroxocobalamin (Alvarez et al. 2012; Garcia et al. 2010). Transcriptional profiling of the *cas-c1* mutant reveals that the genes encoding enzymes involved in cell wall rebuilding and root hair formation are underexpressed in the mutant, as are certain genes involved in ethylene signaling and metabolism (Garcia et al. 2010).

Root hairs are tubular extensions of root epidermal cells produced in the differentiation zone of the root and confer the ability to absorb nutrients and water, interact with microbes, and physically anchor the plant to the soil. Due to the biological importance of these structures, which are also a model for studying tip growth in plants, the molecular mechanisms involved in the specification, differentiation, and physiology of root hairs in *Arabidopsis* have been extensively reviewed (Carol and Dolan 2002; Grierson et al. 2014; Ishida et al. 2008). Root hair specification is determined by position-dependent signaling and molecular feedback loops. Once an initiation site has been selected, cell polarity is established, and a small swelling forms. Root hair elongation relies on polarized cell expansion at the growing tip, which involves multiple integrated processes, including cell secretion, endomembrane trafficking, cytoskeletal organization, and cell wall modifications. Sustained root tip growth involves oscillations in extracellular pH, ROS and cytosolic calcium (Monshausen et al. 2007). Elongation is accompanied by generation of a tip-high calcium gradient that can be observed throughout the remainder of root hair growth (Dolan et al. 1994; Samaj et al. 2004; Schiefelbein et al. 1992; Wymer et al. 1997). Thus, ROS are required for the activation of calcium channels and calcium activates NADPH oxidase in a system of positive feedback that maintains cell polarity during root hair elongation (Gapper and Dolan 2006; Takeda et al. 2008). The genes involved in each of the phases of root hair development have been identified, including transcription factors, cell wall-modifying enzymes, protein from the secretion apparatus, and proteins related to Ca^{2+} production, ROS generation and management, cytoskeleton, etc. (reviewed in (Carol and Dolan 2002; Grierson and Schiefelbein 2009)). Hormones also play a role in root hair development, principally auxin

and ethylene ((Grierson et al. 2014) and references therein).

The goal of this work is to further our understanding of the role of CAS-C1 and cyanide in root hair development. To this end, a cellular strategy was implemented to observe the spatiotemporal expression and subcellular localization of CAS-C1, with a particular focus on developing root hairs. Mutations in the *SUPERCENTIPEDE1* (*SCN1)* gene affect very early steps of the root hair development, resulting in root hair bulges that do not elongate. The SCN1 protein is a Rho GTPase GDP dissociation inhibitor that functions as a negative regulator of Rho-related plant GTPases (ROPs). Throughout hair development, ROP GTPases ROP2, ROP4 and ROP6 localize to the earliest swelling of the basal region and tip. ROPs regulate the activity of the NADPH oxidase encoded by *ROOT HAIR DEFECTIVE 2* (*RHD2*)/*AtrbohC,* which catalyzes the generation of ROS and participates in the generation of the Ca^{2+} gradient at the tip of the root hair that drives root hair elongation (Foreman et al. 2003; Ishida et al. 2008; Jones et al. 2007). Indeed, SCN1 acts on the root hair initiation, swelling formation, transition to tip growth and tip growth steps of root hair formation (Foreman and Dolan 2001; Parker et al. 2000). In *scn1* mutants, ROP2 is mislocalized, and supernumerary hair initiation sites are formed that do not elongate (Carol et al. 2005). Mutants on *rhd2*, on his part, are not able to produce superoxide anion and show abnormal short root hairs (Foreman et al. 2003).

To demonstrate epistatic relationships in the root hair elongation process, genetic crosses between the *cas-c1* mutant and *scn1* or *rhd2* mutants have been performed, and some clues regarding the underlying mechanisms are discussed.

Results

CAS-C1 localizes to mitochondria and accumulates in root hair tips

Based on its sequence and the capacity of the N-terminal portion of the protein to direct the green fluorescent protein (GFP) to mitochondria in transient expression experiments (Yamaguchi et al. 2000), CAS-C1 has been classified as a mitochondrial protein. Aiming to better unravel the role of CAS-C1 in relation to its spatio-temporal expression, we constructed a promoter-genomic open reading frame (ORF)-GFP construct and transformed plants as described in the Materials and Methods section and schematized in Supplementary Fig. S1. We assumed that the intergenic *PIP1-CAS-C1* region should contain all transcriptional regulatory signals for

CAS-C1 expression and that the genomic *CAS-C1* region, from +1 to the STOP codon, should contain the regulatory sequences for the subcellular location of the protein as well as possible additional transcriptional regulatory elements (Gutierrez-Alcala et al. 2005). A translational fusion was then obtained by joining 2676 bp of the genomic sequence containing 1442 bp of the complete intergenic *PIP1-CAS-C1* region plus 1234 bp from the *CAS-C1* ATG to the GAT before the STOP codon (Supplementary Fig. S1, www.arabidopsis.org), to the *GFP* gene carried on the *pMDC110* Gateway vector. The plant transformation construct was named *ProC1:CASC1-GFP*. Transgenic plants were obtained in different backgrounds, the wild type (8 independent lines) and the *cas-c1* (3 independent lines), *scn1-1* (2 independent lines) and *rhd2GK* (6 independent lines) mutants, and analyzed by confocal microscopy for *in vivo* GFP detection. No relevant differences of intensity or localization of the fluorescence were observed among the different lines in any case, so one T3 line of each genotype was selected for further studies.

The spatio-temporal expression of CAS-C1 was examined by observing the fluorescence in different tissues of wild type Arabidopsis plants transformed with the *ProC1:CASC1-GFP* construct. Root tissues presented a homogeneous dotted pattern of fluorescence in wild type background (Fig. 1A, D, G), which was consistent with a mitochondrial localization of the fusion protein. This was confirmed by co-localization of GFP fluorescence with the mitochondrion-specific dye Mitotracker Deep Red 633 (Supplementary Fig. S2). In the root, the signal was very intense, especially in the meristematic zone (Fig. 1A, B, C), likely due to the high mitochondria concentration in cells that are metabolically active. In the root hair, a strong fluorescence at the tip was observed in wild type background (Fig. 1D, G), following the apical growth characteristic of root hairs (Supplementary Video S1). This apical localization of the fluorescence was detected from the very beginning of root hair development, at the swelling region in the initiation stage to the tip of the well-formed root hair (Supplementary Video S1). These results were consistent with the proposed role of CAS-C1 in root hair formation by modulating the accumulation of cyanide present in the growing tip (Garcia et al. 2010), which would act as a repressor of this process from the initial steps. Interestingly, transformation of *cas-c1* mutant plants with the *ProC1:CASC1-GFP* construct reverted, although partially, the root hairless phenotype (Supplementary Fig. S3), showing the complemented line accumulation of GFP in the root hair tip as in wild type background (Supplementary Fig. S3 B, C).

Furthermore, we observed that in the *scn1-1* mutant, despite being unable to produce root hair primordia, the *ProC1:CASC1*-driven GFP fluorescence was localized in the mitochondria, yet in root hairs it did not show a preferential localization of accumulation at the tips of the root hair primordia (Fig. 1B, E, H). Therefore, the

scn1-1 mutation does not affect the subcellular localization of *CAS-C1* but rather to the polarized location of mitochondria at the tip of the developing hair. Similarly, in a T-DNA insertion root hair-specific NADPH oxidase *rhd2* mutant, *rhd2GK*, the fluorescence was localized at the mitochondria as well, although it did not show a root hair tip specific localization (Fig. 1C, F, I).

Therefore, our data were consistent with previous work showing that mitochondria are present at a high density in tip-growing cells and spatially associated with the initiation and elongation of the root hair bulge (Carol and Dolan 2002; Wang et al. 2010). Since cyanide is a potent inhibitor of the cytochrome respiration pathway and root hair elongation is a rapid cell expansion process with high cost of energy, we analyzed whether the increase in cyanide in *cas-c1* mutants could have a detrimental effect because of his presumed inhibition of the energy source required for rapid tip growth. Previous report has shown that neither the respiration rate is diminished, nor the localization of mitochondria is altered within the root hair in the *cas-c1* mutant compared to wild type (García et al 2010). However, we have further analyzed the levels of the main energy source, ATP, in wild type and *cas-c1* mutants in order to ensure that the energy source is not lacking in the *cas-c1* roots. Table 1 shows that ATP levels were indistinguishable in wild type and *cas-c1* mutants, thus ruling out a deleterious effect of cyanide on the production of the energy source required for root hair growth. This result leads us to deepen the concept of cyanide and/or CAS as an independent signaling component in root hair development.

cas-c1 *mutation is hypostatic to the* scn1-1 *and epistatic to the* rhd2-1 *morphological phenotypes*

As CAS-C1 appears to be involved in the regulation of the root hair growth, we further examined the existence of a relationship between CAS-C1 and the root hair elongation pathway. To establish the genetic epistasis between them, genetic crosses were carried out between *scn1-1* (Parker et al. 2000) or *rhd2-1* (Foreman et al. 2003) and *cas-c1* mutants. Double *scn1-1 cas-c1* and *rhd2-1 cas-c1* mutants were generated and confirmed by sequence and PCR analyses (Supplementary Fig. S4 and S5). Root pictures of wild type, parental mutants and the double *scn1-1 cas-c1* and *rhd2-1 cas-c1* mutants at 6-7 d after sowing were captured under a microscope (Fig. 2). The root hairs of the *cas-c1* mutant correctly began to grow and developed small bulges (Fig. 2B, F), and *scn1-1* displayed multiple sites of hair growth emerging from hair-forming cells (Fig. 2C) and *rhd2-1* showed short malformed root hairs (Fig. 2G). The double *scn1-1 cas-c1* mutant exhibited a phenotype that was indistinguishable from that of the *scn1-1* simple mutant, showing multiple root hair primordia that did not elongate (Fig. 2D), whereas the double *rhd2-1 cas-c1* mutant exhibited a phenotype identical to the *cas-c1*

simple mutant, i.e., small protuberances rather than short root hairs, more sparse than in the *rhd2-1* mutant (Fig. 2H). This reveals a role of *CAS-C1* in an intermediate point between *scn1* and the NADPH oxidase action in the root hair elongation process. Addition of the ethylene donor ACC to the culture medium did not elongate root hair cells in any of the single *cas-c1* or double *rhd2-1 cas-c1* or *scn1-1 cas-c1* mutants, demonstrating the independence of *cas-c1* mutation and ethylene production (Supplementary Fig. S6), (Garcia et al. 2010).

In addition, we took advantage of the use of the 2-hydroxocobalamin (COB) compound as an antidote for cyanide poisoning because it reacts with free cyanide, producing cyanocobalamin, or vitamin B12, which is not toxic (Borron et al., 2007; Hall et al., 2007). Addition of COB to the culture medium has no effect on the wild-type root but is able to partially complement the loss-of-hair phenotype of the *cas-c1* mutant (Garcia et al. 2010). By comparing the phenotypes of COB-treated plants, we found that *cas-c1* could partially recover the development of root hairs, as previously reported, but that neither the *scn1-1* nor the double *scn1-1 cas-c1* mutants showed even partial reversion of their loss of the root hair elongation phenotype (Fig. 3C *versus* 3G, 3D *versus* 3H). These findings suggest that cyanide accumulation as the result of *cas-c1* loss-of-function is not involved in the *scn1-1* phenotype. On the other hand, COB treatment was able to revert the hairless root phenotype of the double mutant *rhd2-1 cas-c1* to the single *rhd2-1* mutant (Fig. 3L *versus* 3P), but COB did not revert the *rhd2-1* mutant phenotype (Fig. 3K *versus* 3O) under the conditions tested.

The above observations were supported by further molecular data. Cyanide accumulation in the *cas-c1* mutant has been described to repress several genes encoding enzymes involved in the formation of the root hair tip, mainly cell wall-related proteins including *FLA6* and *MRH5*, an arabinogalactan protein and a glycerophosphoryl diester phosphodiesterase-like GPI-anchored protein respectively (Garcia et al. 2010). Root hair growth includes a variety of cellular components and compounds that work in concert (Carol and Dolan 2002); Mendrinna and Persson 2015). The basic helix-loop-helix (bHLH) transcription factor (TF) ROOT HAIR DEFECTIVE 6 RHD6 controls the initiation of the root hair (Grierson et al. 2014) whereas the bHLH TF RHD6-LIKE 4 RSL4 is a direct transcriptional target of RHD6, and it has been described to integrate the developmental program aiming to regulate the polar growth (Marzol et al., 2017, Vijayakumar et al., 2016). In order to deepen in the epistatic relationships between *cas-c1* and *scn1* or *rhd2*, real-time quantitative RT-PCR was conducted. Figure 4 shows that all genes analyzed were down-regulated in *cas-c1*, *scn1-1* and *rhd2-1* mutants when compared to wild type. When comparing the double *scn1-1 cas-c1* mutant with the single *scn1-1* mutant, we could appreciate that there were no further repression of *RHD6*, *RSL4* or *MHR5* and only a slight repression of *FLA6* (Fig. 4A). This suggests that the *cas-c1* mutation did not significantly affect the behavior of

the single *scn1-1* mutation at the molecular level, and further supports the epistasy of the *scn1-1* mutation to *cas-c1*. On the other hand, in the *rhd2-1* background, the *cas-c1* mutation diminished further the *RHD6*, *MHR5* and, in a lesser extent, *RSL4* gene expression and thus we could observe an additional repression of these genes in the *rhd2-1 cas-c1* mutant compared to the single *rhd2-1* single mutant (Fig. 4B), meaning that the *cas-c1* mutation was epistatic to *rhd2-1* also at the molecular level. *FLA6* expression was unchanged in the double *rhd2-1 cas-c1* mutant *versus* the single *rhd2-1* mutant (Fig. 4B).

Finally, it is interesting to note that in both *scn1-1 cas-c1* and *rhd2-1 cas-c1* double mutant roots the cyanide content increased 55 % and 33 % respectively compared to their parental backgrounds (that is, the single *scn1-1* and the single *rhd2-1* mutant roots, respectively), similarly to the increase of 39 % of cyanide content in roots of *cas-c1* compared to the wild type (Supplementary Fig. S7). This indicates that CAS-C1 is active in single *scn1-1* and *rhd2-1* mutants.

Cyanide effect on root hair elongation is independent of H_2O_2 production and of direct NADPH oxidase inhibition

In *Arabidopsis*, the NADPH oxidase Rhd2/AtrbohC produces superoxide anion ($O_2^{\bullet-}$) in the root hair (Torres et al., 1998). Root hairs in the *rhd2* mutants do not accumulate $O_2^{\bullet-}$ and form swellings instead of elongating (Schiefelbein and Somerville 1990). Therefore, root hair elongation is driven in part by accumulation of $O_2^{\bullet-}$ at the tip of the root hair. When superoxide anion was detected by specific nitro blue tetrazolium (NBT) staining in the root, we observed that $O_2^{\bullet-}$ did not accumulate in the *cas-c1* mutant in comparison to wild type ((Garcia et al. 2010) and Fig. 5A-B), as it has been described for the *rhd2-1* mutant (Carol et al. 2005). In contrast, it was present at ectopic foci and over a greater area of the cell surface in both *scn1-1* ((Carol et al. 2005), Fig. 5C) and double *scn1-1 cas-c1* (Fig. 5D) mutants than in wild type plants. This result confirms that SCN may act upstream of or independently from CAS-C1 in regulating root hair growth and also suggests that NADPH oxidase is not sensitive to the concentration of cyanide that accumulates in *cas-c1*, as $O_2^{\bullet-}$ accumulated in the double *scn1-1 cas-c1* mutant despite the *cas-c1* mutation (Fig. 5D). The *rhd2-1* mutant does not produce $O_2^{\bullet-}$ in root hairs and consequently it does not show any NBT staining in root hairs (Foreman et al., 2003; Carol et al., 2005), just like *cas-c1* (García et al., 2010), therefore the double *rhd2-1 cas-c1* mutant didn't show NBT staining at his root hair tips (Fig. 5E-F).

To further investigate the effect of cyanide in the NADPH oxidase activity, this activity was measured in root

protein extracts in the presence or absence of KCN 0.1 mM. The NADPH oxidase activity was unchanged regardless of the presence or the absence of KCN (Table 2). Moreover, NADPH oxidase activity was unchanged in wild type and *cas-c1* mutant roots (Table 2). Collectively, these results confirmed that the NADPH oxidase is insensitive to cyanide.

Other ROS act in root hair development, and it has been demonstrated that H_2O_2 participates in the regulation of root hair formation (Sundaravelpandian et al. 2013b; Zhao et al. 2016). To further understand the relationship between other ROS and the mutation in *cas-c1*, we performed H_2O_2 staining with 2',7'-dichlorodihydrofluorescein diacetate (H_2DCFDA) of single and double mutants (Fig. 6). 14-d-old roots revealed higher accumulation of H_2O_2 in the elongation zone of *cas-c1* and *scn1-1 cas-c1* than in wild type and the *scn1-1* mutant (Garcia et al. 2010); Fig. 6 B, E), even though no significant staining was observed in the root hairs. Neither the single *rhd2-1* nor the double *rhd2-1 cas-c1* mutants showed H_2O_2 staining at the elongation zone, although the latter show a clear *cas-c1* phenotype (Fig. 2 H), supporting the hypothesis the effect of cyanide in root hair elongation is independent of ROS production.

Discussion

The results presented in this article deepen our understanding of the role of the mitochondrial ß-cyanoalanine synthase CAS-C1 in root hair development. In a previous report (Yamaguchi et al. 2000), the mitochondrial localization of this protein was observed by transiently expressing a fusion between the strong constitutive 35S promoter and a cDNA fragment encoding the CAS-C1 N-terminus with GFP in Arabidopsis. Instead, our strategy attempted to emulate as much as possible the *in vivo* situation by fusing the *CAS-C1* promoter and the genomic coding sequence to GFP. With this approach, we obtained spatiotemporal information about *CAS-C1* regulation (driven by signals present in the promoter and other regulatory regions) and localization (driven by signals present in the coding sequence). We confirmed that CAS-C1 is localized to mitochondria, and we followed its tip-preferred localization during root hair growth. Root hair growth is a highly polarized process allowing growth only at the tip and not along the shanks. Polar growth involves cytoplasmic streamings that transport vesicles containing the cargo molecules necessary for cellular growth, such as cell wall polysaccharides, proteins and glycoproteins, which will be incorporated into the newly forming cell wall (Balcerowicz et al. 2015; Carol and Dolan 2002; Datta et al. 2011; Grierson et al. 2014; Ketelaar 2013; Salazar-Henao and Schmidt 2016). These vesicles, located in the tip zone, are produced by the endoplasmic reticulum

and Golgi complexes, and are directed to the tip by processes that depend on pH, ROS and calcium gradient oscillations as well as the cytoskeleton (Datta et al. 2011; Grierson et al. 2014; Ishida et al. 2008; Salazar-Henao and Schmidt 2016; Schiefelbein et al. 1992). An organelle-rich region, comprising the Golgi complex, endoplasmic reticulum and mitochondria, occurs in the sub-apical zone (Carol and Dolan 2002; Datta et al. 2011; Foreman and Dolan 2001). In addition to providing the energy needed for active transport, mitochondria serve as important Ca^{2+} stores and are able to move along the cytoskeleton to provide Ca^{2+} to sustain root hair elongation (Libault et al. 2010; Wang et al. 2010). Our previous work (Garcia et al. 2010) and this study suggest that root hair mitochondria are also essential for maintaining the proper level of cyanide at the root hair tip for elongation. SCN1 is essential for properly localization NADPH oxidase RHD2 at the root hair tip. In the *scn1-1* mutant, the specific localization of $O_2^{\bullet-}$ at the tip of the root hairs is not observed and the tip growth of root hair does not occur (Carol et al. 2005; Foreman et al. 2003; Ishida et al. 2008; Jones et al. 2007). The lack of tip-polarized mitochondria in the *scn1-1* and in the *rhd2-1* mutants suggests that SCN1 and RHD2 participate in the localization of this organelle during root hair formation.

The *ProC1:CASC1-GFP* construct was able to revert the root hairless phenotype of *cas-c1*, although partially. Partial reversion is also observed when the CaMV35S promoter is used (García et al., 2010) and it can be explained either by a positional effect or by lack of transcriptional signals in the intergenic region that we have considered should contain the whole promoter. Another possibility is that the CASC1-GFP chimeric protein shows a reduced activity compared to the native CAS-C1.

We have demonstrated that *scn1-1* mutation is epistatic to *cas-c1* and *cas-c1* is epistatic to *rhd2-1* through genetic experiments, as the *cas-c1* phenotype is not seen when combined with *scn1-1* but it is dominant to the *rhd2-1* phenotype. Also, treatment with the antidote COB did not complement the non-elongated root hair phenotype of the *scn1-1 cas-c1* double mutant as it does in the case of the *cas-c1* mutant or in the double mutant *rhd2-1 cas-c1* ((Garcia et al. 2010); this work). Therefore, the target of cyanide should be either not present or not active in *scn1-1* mutants, thereby avoiding the cyanide repressor effect. On the other hand, COB rescues the double *rhd2-1 cas-c1* mutant to a single *rhd2-1* phenotype, suggesting that the target of cyanide should be present in the *rhd2-1* mutant, so excluding the ATRBOHC NADPH oxidase as a main target. Moreover, quantitative RT-PCR analysis of several genes involved in the early (*RHD6* and *RSL4*) or late (*MRH5* and *FLA6*) steps of the root hair elongation indicate that all of them are transcriptionally repressed in the *cas-c1* mutant thus suggesting that the cyanide action should be exerted at the beginning of the root hair elongation process. Moreover, the fact that the *cas-c1* mutation has no effect on the transcriptional regulation of most of the root hair

genes analyzed in *scn1-1* genetic background while it decreases its transcription in *rhd2-1* genetic background supports the proposed epistatic relationships.

The phenotype of the *scn1-1* mutant is completely different from that of the *cas-c1* mutant: in the first case, supernumerary chubby and short root hairs are produced; in the second case, root hairs are scarce, short and have a crushed look, similar but more penetrant to that exhibited by NADPH oxidase AtRBOHC/*RHD2* mutants (Carol and Dolan 2006; Foreman et al. 2003). Taking into consideration that SCN1 should act before ATRBOHC/RHD2 (Grierson et al. 2014; Parker et al. 2000), and that CAS-C1 may act before ATRBOHC/RHD2, we cannot entirely exclude the possibility that cyanide could anyway repress ATRBOHC through the formation of a complex with its heminic iron. Although there are no previous *in vitro* data regarding the sensitivity of this NADPH oxidase or any member of its family, these enzymes are more resistant to cyanide than peroxidases, which is a criterion for discerning between the two activities (Bolwell et al. 1998). According to NBT staining, it does not appear to be plausible that cyanide acts by inhibiting AtRBOHC activity, as the double *scn1-1 cas-c1* mutant accumulated $O_2^{\bullet-}$ at the same level as the single *scn1-1* mutant, despite the *cas-c1* mutation. Moreover, our biochemical studies have definitely shown that the root NADPH oxidase activity is not sensitive to KCN.

The redox state of the cell is crucial for cell cycle progression (Tsukagoshi et al. 2010), however the role of H_2O_2 in root hair formation is controversial. A balance between $O_2^{\bullet-}$ and H_2O_2 is crucial for the transition from proliferation to differentiation in the *A. thaliana* root (Sundaravelpandian et al. 2013a; Sundaravelpandian et al. 2013b; Tsukagoshi et al. 2010). In this organ, although $O_2^{\bullet-}$ is predominantly located in the apoplast of the cell elongation zone, H_2O_2 accumulates in the differentiation zone and the cell walls of root hairs during formation, suggesting a role in different stages of root hair formation (Dunand et al. 2007; Zhao et al. 2016). Indeed, treatments that decreased the $O_2^{\bullet-}$ concentration also reduce root elongation and root hair formation, whereas H_2O_2 scavenging promotes root elongation and suppresses root hair formation (Dunand et al. 2007). Furthermore, H_2O_2 is required for peroxidase-mediated local disassembly of the cell wall to initiate bulge formation and for cell wall remodeling during the later stages of root hair development (Kwasniewski et al. 2013; Takeda et al. 2008). If the higher H_2O_2 content in the roots of the *cas-c1* and double *scn1-1 cas-c1* mutants is related to root hair formation, these mutants should have long root hairs compared to wild type or the *scn1-1* mutant, as this ROS has been associated with promoting root hair elongation rather than impeding its development (Dunand et al. 2007; Zhao et al. 2016). Moreover, the double *rhd2-1 cas-c1* mutant display low levels of H_2O_2 accumulation in the elongation zone although its phenotype is indistinguishable from the *cas-c1*

mutant, thus uncoupling ROS accumulation to *cas-c1* mutation. Our results confirm that the role of CAS-C1 in root hair development extends the mere detoxification of a non-specific poison (cyanide) that produces general oxidative stress in roots and interferes with appropriate root hair generation. Instead, CAS-C1 appears to detoxify cyanide, which has a specific target, and cyanide signaling is independent of ROS. The precise mechanism(s) by which cyanide affects root hair development requires further research; nonetheless this work demonstrates that the mechanism certainly is independent of ROS production and that it is genetically positioned at the first steps of root hair elongation, after root hair cell fate determination, between the SCN1 action and the $O_2^{\bullet-}$ production by RHD2. The current working model (Fig. 7) needs to determine which protein(s) or factor(s) are affected by cyanide and the underlying molecular mechanisms.

Materials and Methods

Plant material and growth conditions

Arabidopsis (*Arabidopsis thaliana*) wild-type ecotype Col-0, and *cas-c1* (SALK_022479) (Garcia et al. 2010), *scn1-1* (Carol et al. 2005), *rhd2-1* (Foreman et al. 2003) and *rhd2GK* (GK_841E09.01) mutants were used in this work.

Arabidopsis seeds were surface-sterilized and synchronized at 4°C for 4 d. Plants were grown on solid MS medium containing 0.8% or 3.5% (w/v) agar or phytagel, respectively, and 1% (w/v) sucrose in vertical Petri dishes under a photoperiod of 16 h of white light (120 µE m^{-2} s^{-1}) at 20ºC/8 h dark at 18ºC.

For hydroxocobalamin (COB) treatment, the seedlings were germinated on Murashige and Skoog (MS) containing 5 mM COB (Sigma-Aldrich) and grown for 4 d. For Nitroblue tetrazolium (NBT) staining, seedlings were germinated in MS medium for 3 d. For RT-qPCR and phenotype imaging, *rhd2-1* and *rhd2-1 cas-c1* mutant seedlings were grown in MS medium at pH 4 to optimize the visualization of the phenotype.

For 1-aminocyclopropane-1-carboxylic acid (ACC) treatment, the seedlings were germinated on Murashige and Skoog (MS) containing 50 mM ACC (Sigma-Aldrich) and grown for 14 d on vertical plates.

DNA cloning and plasmid construction

To clone the promoter and ORF of the *CAS-C1* (At3g61440) gene, a 2.7 kb of the genomic sequence was amplified using specific primers. Total DNA was isolated from young Arabidopsis leaves using the Qiagen DNeasy Plant Mini kit. The 2.7 kb sequence containing the intergenic *PIP1-CAS-C1* sequence and the ORF of the *CAS-C1* gene was amplified by PCR using the primers pC1-C1-F: 5´-CACCGTAAAAACAAGACATCAAGTCCTCTG-3´ and pC1-C1-R: 5´-ATCCACTGAAACTGGCTTCA-3´ and the Invitrogen proofreading Platinum Pfx DNA polymerase. The PCR conditions were as follows: a denaturation cycle of 2 min at 94ºC, followed by 30 amplification cycles of 15 s at 94ºC, 30 s at 55ºC, and 1 min at 68ºC. The amplified region was then ligated to the Invitrogen pENTR/D-TOPO vector using the Invitrogen Directional TOPO Cloning Kit following the manufacturer's instructions. Positive clones were identified by colony PCR and DNA restriction analysis. Using Invitrogen Gateway® technology, the *CAS-C1* promoter and ORF were then cloned into the pMDC110 vector (Curtis and Grossniklaus 2003), a plant expression vector for the construction of promoter-reporter GFP plasmids. The final construct used for plant transformation was identified by colony PCR and sequencing. The plasmid was named *ProC1:CASC1-GFP*.

Transformation of Arabidopsis

For plant transformation, the construct *ProC1:CASC1-GFP* was transformed into *Agrobacterium tumefaciens* and then introduced into *A. thaliana* plants by dipping the developing floral tissues into a solution containing the transformed *A. tumefaciens* strain, 5% sucrose, and 0.005% (v/v) of the surfactant SilwetL-77 (Clough and Bent 1998). Transgenic plants were recovered by selecting seeds on solid MS medium containing 20 mg/L of hygromycin. In the case of *rhd2GK* transformed with *ProC1:CASC1-GFP*, the selection media contained 15 mg/l of hygromycin plus 5 mg/L of sufadiazine.

GFP detection by confocal microscopy

Tissues from transgenic Arabidopsis plants were imaged using a Leica TCS SP2 spectral confocal microscope. Samples were excited using an argon ion laser at 488 nm; emission was detected between 510 and 580 nm for GFP imaging (pseudocolored green). The microscopy images were processed using Leica Confocal Software.

Mitochondria staining

Root tissues were incubated with a 20 nM solution of MitoTracker Deep Red (Molecular Probes) for 10 min at room temperature. Samples were observed using a Leica HCX PLAN-APO 363 1.4 NA oil immersion objective with a Leica TCS SP2 spectral confocal microscope (Leica Microsystems). The dye was excited using a helium-neon laser at 644 nm, either in single confocal optical sections or in serial optical sections. Emitted light was collected through a triple dichroic beam splitter (TD 488/543/633) and detected after spectral separation in the 650 to 700 nm range (pseudocolored blue).

Detection of ROS

For detection of the superoxide anion, roots were stained with NBT (Nitrotetrazolium blue chloride, Sigma-Aldrich) as described previously (Garcia et al. 2010). Seedlings were incubated in 0.1 M Tris-HCl, 0.1 M NaCl, 0.05 M $MgCl_2$, and 0.5 mg mL^{-1} NBT (pH 9.5) for 2 h at room temperature in the dark. After rinsing, roots were imaged under bright-field illumination under an Olympus BX50 microscope and images were taken using a Leica DFC300FX digital camera.

For fluorimetric detection of H_2O_2, roots were incubated for 5 min with 10 mM H_2DCFDA (Life Technologies) in the presence of 10 mM propidium iodide (Life Technologies) to visualize cell walls. The samples were observed using a TCS SP2 spectral confocal microscope (Leica Microsystems) with the following settings: excitation, 488 nm; emission, 500 to 550 nm for fluorescein detection and 600 to 650 nm for propidium iodide detection.

Real-time RT-PCR

Quantitative real-time RT-PCR was used to analyze the expression of the *MHR5*, *FLA6*, *RHD6* and *RSL4* genes. Total RNA was extracted from Arabidopsis leaves using the Qiagen RNeasy Plant Mini Kit. RNA was reverse transcribed using an oligo (dT) primer and Invitrogen Super-script First-Strand Synthesis System for RT-PCR following the manufacturer's instructions. Gene-specific primers for each gene were designed using the Invitrogen Vector NTI Advance 10 software. The primer sequences were as follows: QFMRH5, 5′-GCTGCTTGCTGCTCAAATCC-3′ and *QRMRH5*, 5′-AATCCAGAGAATCCACCACG-3′ for the *MRH5* gene; QFFLA6, 5′-CAAATCCAGCTCATGCTCTACC-3′ and QRFLA6, 5′-TCTTGTCCCGTAGCCTGAGT-

3′ for *FLA6* gene; qRHD6-Fw, 5′- CCGGCTCAAGGAGGAAAA-3′ and qRHD6-R, 5′- CGAATTCCTGTCTCGTTGTGA-3′ for *RHD6* gene; qRSL4-Fw, 5′- CAGATTAAGTTGTTGAGCTCGG-3′ and qRSL4-R, 5′- GAGACAAAAGGTTGTGATGGAA-3′ for *RSL4* gene; qUbq10-F, 5′- GGCCTTGTATAATCCCTGATGAATAAG-3′ and qUbq10-R, 5′- AAAGAGATAACAGGAACGGAAACATAGT-3′ for the constitutive *UBQ10* gene. Real-time PCR was performed using the Bio-Rad IQ SYBR Green Supermix. Signals were detected with a Bio-Rad iCYCLER according to the manufacturer's instructions. The cycling profile consisted of 95°C for 10 min followed by 45 cycles of 95°C for 15 s and 60°C for 1 min. A melting curve from 60°C to 90°C was performed following PCR cycling. The expression levels of genes of interest were normalized to that of the constitutive UBQ10 gene by subtracting the cycle threshold (CT) value of *UBQ10* from that of the gene of interest (ΔCT) and calculated as $2^{-\Delta CT}$. The results shown are the means ± SD of at least three independent RNA samples.

Determination of ATP

The adenine triphosphate in the roots was extracted following the boiling water method (Yang et al. 2002). Briefly, 50 mg of root tissues were mixed with 100 µl of ice-cold distilled H_2O, which was immediately heated in a boiling water bath for 10 min (Li et al. 2017). The boiled lysates were centrifuged at 15,000 g for 5 min at 4 ºC and the supernatants were collected for ATP measurement using an ATP Determination kit (A22066, ThermoFisher Scientific®), following the manufacturer's protocol in a Thermo Scientific Varioskan® Flash.

Cyanide determination by high-performance liquid chromatography (HPLC)

A total of 100 mg of root tissue was homogenized in liquid nitrogen using a mortar and pestle and resuspended in cold borate-phosphate extraction buffer (2 mL g^{-1} fresh weight) containing 27 mM sodium borate and 47 mM potassium phosphate, pH 8.0. The homogenates were centrifuged at 15,000 g for 15 min at 4°C. Extracted cyanide was subsequently quantified by reverse-phase HPLC after derivatization with 2,3-naphthalenedialdehyde to form a 1-cyano-2-alkyl-benz[f]isoindole derivative using previously described methods (Garcia et al. 2010; Lin et al. 2005).

Determination of NADPH oxidase activity

NADPH activity in root extracts was measured using a method adapted from a previous report (Kaundal et al. 2012). Frozen roots (50 mg) were homogenized in 1 ml of 50 mM HEPES buffer (pH 7.2) containing 0.25 M sucrose, 3 mM EDTA, 1 mM dithiotreitol (DTT), 3.6 mM L-cysteine, 0.1 mM $MgCl_2$ and 0.6% polyvinylpyrrolidone (PVP) with the addition of Complete Protease Inhibitor Cocktail Tablets (Sigma). The homogenate tissue was filtered through two layers of Miracloth and centrifuged at 10,000 x g for 45 min at 4ºC. The supernatant was centrifuged at 203,000 g for 60 min at 4ºC. The pellet was resuspended in 150 µl ice-cold 10 mM Tris-HCl (pH 7.4) and used for the enzyme assay. NADPH oxidase activity was assayed colorimetrically with XTT (3′-[1-[(phenylamino)-carbony]-3,4-tetrazolium]-bis(4-methoxy-6-nitro)benzene-sulfonic acid) sodium salt as a substrate. The reaction mixture contained 50 mM Tris-HCl buffer (pH 7.5), 0.5 mM XTT, 0.1 mM NADPH and 5 µg protein extract. The linear increase in absorption at 492 nm due to the formation of a yellow formazan was followed for 120 min (extinction coefficient of 21.6 mM^{-1} cm^{-1}).

Funding

This work was supported in part by the European Regional Development Fund through Ministerio de Economía y Competitividad [grant MOLCYS, no. BIO2013-44648-P] and Agencia Estatal de Investigación [grant no. BIO2016-76633-P] L.A.-A. thanks the Ministerio de Economía y Competitividad for fellowship support through the program of Formación de Personal Investigador.

Acknowledgments

We thank Dr. Alicia Orea for confocal microscopy service and Inmaculada Moreno for technical assistance.

References

Alvarez, C., Garcia, I., Romero, L.C. and Gotor, C. (2012) Mitochondrial sulfide detoxification requires a functional isoform O-acetylserine(thiol)lyase C in Arabidopsis thaliana. *Mol Plant* 5: 1217-1226.

Balcerowicz, D., Schoenaers, S. and Vissenberg, K. (2015) Cell Fate Determination and the Switch from Diffuse Growth to Planar Polarity in Arabidopsis Root Epidermal Cells. *Front Plant Sci* 6: 1163.

Bethke, P.C., Libourel, I.G., Reinohl, V. and Jones, R.L. (2006) Sodium nitroprusside, cyanide, nitrite, and nitrate break Arabidopsis seed dormancy in a nitric oxide-dependent manner. *Planta* 223: 805-812.

Bleecker, A.B. and Kende, H. (2000) Ethylene: a gaseous signal molecule in plants. *Annu. Rev. Cell. Dev. Biol.* 16: 1-18.
Bolwell, G.P., Davies, D.R., Gerrish, C., Auh, C.K. and Murphy, T.M. (1998) Comparative biochemistry of the oxidative burst produced by rose and French bean cells reveals two distinct mechanisms. *Plant Physiol.* 116: 1379-1385.
Carol, R.J. and Dolan, L. (2002) Building a hair: tip growth in Arabidopsis thaliana root hairs. *Philos Trans R Soc Lond B Biol Sci* 357: 815-821.
Carol, R.J. and Dolan, L. (2006) The role of reactive oxygen species in cell growth: lessons from root hairs. *J. Exp. Bot.* 57: 1829-1834.
Carol, R.J., Takeda, S., Linstead, P., Durrant, M.C., Kakesova, H., Derbyshire, P., et al. (2005) A RhoGDP dissociation inhibitor spatially regulates growth in root hair cells. *Nature* 438: 1013-1016.
Chivasa, S. and Carr, J.P. (1998) Cyanide restores N gene-mediated resistance to tobacco mosaic virus in transgenic tobacco expressing salicylic acid hydroxylase. *Plant Cell* 10: 1489-1498.
Cipollone, R. and Visca, P. (2007) Is there evidence that cyanide can act as a neuromodulator? *IUBMB Life* 59: 187-189.
Clough, S.J. and Bent, A.F. (1998) Floral dip: a simplified method for Agrobacterium-mediated transformation of Arabidopsis thaliana. *Plant J.* 16: 735-743.
Cohn, M.A. and Hughes, J.A. (1986) Seed dormancy in red rice. 5. Response to azide, hydroxylamine and cyanide. *Plant Physiol.* 80: 531-533.
Cooper, C.E. and Brown, G.C. (2008) The inhibition of mitochondrial cytochrome oxidase by the gases carbon monoxide, nitric oxide, hydrogen cyanide and hydrogen sulfide: chemical mechanism and physiological significance. *J. Bioenerg. Biomembr.* 40: 533-539.
Curtis, M.D. and Grossniklaus, U. (2003) A gateway cloning vector set for high-throughput functional analysis of genes in planta. *Plant Physiol.* 133: 462-469.
Datta, S., Kim, C.M., Pernas, M., Pires, N.D., Proust, H., Tam, T., et al. (2011) Root hairs: development, growth and evolution at the plant-soil interface. *Plant Soil* 346: 1-14.
Dolan, L., Duckett, C.M., Grierson, C.S., Linstead, P., Schneider, K., Lawson, E., et al. (1994) Clonal relationships and cell patterning in the root epidermis of Arabidopsis. *Development* 120: 2465-2474.
Donato, D.B., Nichols, O., Possingham, H., Moore, M., Ricci, P.F. and Noller, B.N. (2007) A critical review of the effects of gold cyanide-bearing tailings solutions on wildlife. *Environ. Int.* 33: 974-984.
Dunand, C., Crevecoeur, M. and Penel, C. (2007) Distribution of superoxide and hydrogen peroxide in Arabidopsis root and their influence on root development: possible interaction with peroxidases. *New Phytol.* 174: 332-341.
Foreman, J., Demidchik, V., Bothwell, J.H., Mylona, P., Miedema, H., Torres, M.A., et al. (2003) Reactive oxygen species produced by NADPH oxidase regulate plant cell growth. *Nature* 422: 442-446.
Foreman, J. and Dolan, L. (2001) Root Hairs as a Model System for Studying Plant Cell Growth. *Ann. Bot.* 88: 1-7.
Gapper, C. and Dolan, L. (2006) Control of plant development by reactive oxygen species. *Plant Physiol.* 141: 341-345.
Garcia, I., Castellano, J.M., Vioque, B., Solano, R., Gotor, C. and Romero, L.C. (2010) Mitochondrial beta-cyanoalanine synthase is essential for root hair formation in Arabidopsis thaliana. *Plant Cell* 22: 3268-3279.
Garcia, I., Gotor, C. and Romero, L.C. (2014) Beyond toxicity: A regulatory role for mitochondrial cyanide. *Plant Signal. Behav.* 8.

Garcia, I., Rosas, T., Bejarano, E.R., Gotor, C. and Romero, L.C. (2013) Transient transcriptional regulation of the CYS-C1 gene and cyanide accumulation upon pathogen infection in the plant immune response. *Plant Physiol.* 162: 2015-2027.
Glawischnig, E. (2007) Camalexin. *Phytochemistry* 68: 401-406.
Grierson, C., Nielsen, E., Ketelaarc, T. and Schiefelbein, J. (2014) Root hairs. *Arabidopsis Book* 12: e0172.
Grierson, C. and Schiefelbein, J. (2009) Genetics of Root Hair Formation. In *Root Hairs*. Edited by Emons, A.M.C. and Ketelaar, T. pp. 1-25. Springer Berlin Heidelberg, Berlin, Heidelberg.
Gutierrez-Alcala, G., Calo, L., Gros, F., Caissard, J.C., Gotor, C. and Romero, L.C. (2005) A versatile promoter for the expression of proteins in glandular and non-glandular trichomes from a variety of plants. *J. Exp. Bot.* 56: 2487-2494.
Ishida, T., Kurata, T., Okada, K. and Wada, T. (2008) A genetic regulatory network in the development of trichomes and root hairs. *Annu. Rev. Plant Biol.* 59: 365-386.
Jones, M.A., Raymond, M.J., Yang, Z. and Smirnoff, N. (2007) NADPH oxidase-dependent reactive oxygen species formation required for root hair growth depends on ROP GTPase. *J. Exp. Bot.* 58: 1261-1270.
Kaundal, A., Rojas, C.M. and Mysore, K.S. (2012) Measurement of NADPH Oxidase Activity in Plants. *Bio-protocol* 2: e278.
Ketelaar, T. (2013) The actin cytoskeleton in root hairs: all is fine at the tip. *Curr. Opin. Plant Biol.* 16: 749-756.
Kwasniewski, M., Chwialkowska, K., Kwasniewska, J., Kusak, J., Siwinski, K. and Szarejko, I. (2013) Accumulation of peroxidase-related reactive oxygen species in trichoblasts correlates with root hair initiation in barley. *J. Plant Physiol.* 170: 185-195.
Li, F.J., Xu, Z.S., Soo, A.D., Lun, Z.R. and He, C.Y. (2017) ATP-driven and AMPK-independent autophagy in an early branching eukaryotic parasite. *Autophagy* 13: 715-729.
Libault, M., Brechenmacher, L., Cheng, J., Xu, D. and Stacey, G. (2010) Root hair systems biology. *Trends Plant Sci.* 15: 641-650.
Lin, C.C., Wong, B.K., Burgey, C.S., Gibson, C.R. and Singh, R. (2005) In vitro metabolism of a thrombin inhibitor and quantitation of metabolically generated cyanide. *J. Pharm. Biomed. Anal.* 39: 1014-1020.
Machingura, M., Salomon, E., Jez, J.M. and Ebbs, S.D. (2016) The beta-cyanoalanine synthase pathway: beyond cyanide detoxification. *Plant Cell Environ* 39: 2329-2341.
Monshausen, G.B., Bibikova, T.N., Messerli, M.A., Shi, C. and Gilroy, S. (2007) From the Cover: Oscillations in extracellular pH and reactive oxygen species modulate tip growth of Arabidopsis root hairs. *Proc. Natl. Acad. Sci. USA* 104: 20996-21001.
Parker, J.S., Cavell, A.C., Dolan, L., Roberts, K. and Grierson, C.S. (2000) Genetic interactions during root hair morphogenesis in Arabidopsis. *Plant Cell* 12: 1961-1974.
Piotrowski, M. (2008) Primary or secondary? Versatile nitrilases in plant metabolism. *Phytochemistry* 69: 2655-2667.
Romero, L.C., Aroca, M.A., Laureano-Marin, A.M., Moreno, I., Garcia, I. and Gotor, C. (2014) Cysteine and cysteine-related signaling pathways in Arabidopsis thaliana. *Mol Plant* 7: 264-276.
Salazar-Henao, J.E. and Schmidt, W. (2016) An Inventory of Nutrient-Responsive Genes in Arabidopsis Root Hairs. *Front Plant Sci* 7: 237.
Samaj, J., Baluska, F. and Menzel, D. (2004) New signalling molecules regulating root hair tip growth. *Trends Plant Sci.* 9: 217-220.

Schiefelbein, J.W., Shipley, A. and Rowse, P. (1992) Calcium influx at the tip of growing root-hair cells of Arabidopsis thaliana. *Planta* 187: 455-459.
Schiefelbein, J.W. and Somerville, C. (1990) Genetic Control of Root Hair Development in Arabidopsis thaliana. *Plant Cell* 2: 235-243.
Seo, S., Mitsuhara, I., Feng, J., Iwai, T., Hasegawa, M. and Ohashi, Y. (2011) Cyanide, a coproduct of plant hormone ethylene biosynthesis, contributes to the resistance of rice to blast fungus. *Plant Physiol.* 155: 502-514.
Siegien, I. and Bogatek, R. (2006) Cyanide action in plants - from toxic to regulatory. *Acta Physiologiae Plantarum* 28: 483-497.
Sundaravelpandian, K., Chandrika, N., Tsai, Y.H. and Schmidt, W. (2013a) PFT1-controlled ROS balance is critical for multiple stages of root hair development in Arabidopsis. *Plant Signal. Behav.* 8: e24066.
Sundaravelpandian, K., Chandrika, N.N. and Schmidt, W. (2013b) PFT1, a transcriptional Mediator complex subunit, controls root hair differentiation through reactive oxygen species (ROS) distribution in Arabidopsis. *New Phytol.* 197: 151-161.
Takeda, S., Gapper, C., Kaya, H., Bell, E., Kuchitsu, K. and Dolan, L. (2008) Local positive feedback regulation determines cell shape in root hair cells. *Science* 319: 1241-1244.
Tsukagoshi, H., Busch, W. and Benfey, P.N. (2010) Transcriptional regulation of ROS controls transition from proliferation to differentiation in the root. *Cell* 143: 606-616.
Wang, Y., Zhu, Y., Ling, Y., Zhang, H., Liu, P., Baluska, F., et al. (2010) Disruption of actin filaments induces mitochondrial Ca2+ release to the cytoplasm and [Ca2+]c changes in Arabidopsis root hairs. *BMC Plant Biol.* 10: 53.
Watanabe, M., Kusano, M., Oikawa, A., Fukushima, A., Noji, M. and Saito, K. (2008) Physiological roles of the beta-substituted alanine synthase gene family in Arabidopsis. *Plant Physiol.* 146: 310-320.
Wong, C.E., Carson, R.A. and Carr, J.P. (2002) Chemically induced virus resistance in Arabidopsis thaliana is independent of pathogenesis-related protein expression and the NPR1 gene. *Mol Plant Microbe Interact* 15: 75-81.
Wymer, C.L., Bibikova, T.N. and Gilroy, S. (1997) Cytoplasmic free calcium distributions during the development of root hairs of Arabidopsis thaliana. *Plant J.* 12: 427-439.
Yamaguchi, Y., Nakamura, T., Kusano, T. and Sano, H. (2000) Three Arabidopsis genes encoding proteins with differential activities for cysteine synthase and beta-cyanoalanine synthase. *Plant Cell Physiol.* 41: 465-476.
Zhao, P., Sokolov, L.N., Ye, J., Tang, C.Y., Shi, J., Zhen, Y., et al. (2016) The LIKE SEX FOUR2 regulates root development by modulating reactive oxygen species homeostasis in Arabidopsis. *Scientific reports* 6: 28683.

Tables

Plant line	Adenosine triphosphate (nM)
Wild type	400.9 ± 118.6
cas-c1	427.6 ± 118.2

Table 1. Adenosine triphosphate levels in root extracts. The ATP level was determined in crude extracts prepared from the roots of wild type and *cas-c1* mutant plants grown in solid MS medium supplemented with sucrose for 14 d. Values are means ± SD from three independent experiments.

Plant line	NADPH oxidase activity (mU/µg)
wild type	23.23 ± 2.8
cas-c1	20.64 ± 0.6
wild type + KCN 0.1mM	21.09 ± 0.5

Table 2. NADPH oxidase activity level in root extracts. The activity was determined in crude extracts with or without 0.1 mM KCN treatment, prepared from the roots of wild type and mutants grown in solid MS medium supplemented with sucrose for 14 d. Values are means ± SD from five independent experiments.

Legends to figures

Figure 1. *CAS-C1* expression and localization study. Representative GFP images of A,D,G, wild type, B,E,H, *scn1-1* mutant and C,F,I, *rhd2GK* mutant transformed with *ProC1:CASC1-GFP*. Plants were grown in MS medium supplemented with sucrose for 2 days. Images are maximum projection of 20 optical sections.

Figure 2. Root hair phenotypes of root hair formation mutants. (A, E) Wild type, (B, F) *cas-c1*, (C) *scn1-1*, (D) *scn1-1 cas-c1,* (G) *rhd2-1*, *(*H) *rhd2-1 cas-c1* . Seedlings were grown 6-d on MS (A-D) or 7-d on MS pH4 (E-H) medium supplemented with sucrose in vertical plates. Representative images are shown. Bars = 0.5 mm.

Figure 3. Hydroxocobalamin effect on root hair formation. (A-D) Root hair phenotype of wild type, *cas-c1*, *scn1-1* and *scn1-1 cas-c1* 3-d-old plants, respectively, grown on MS sucrose vertical plates in the absence of hydroxocobalamin. (E-H) Root hair phenotype of wild type, *cas-c1*, *scn1-1* and *scn1-1cas-c1* 3-d-old plants, respectively, grown on MS sucrose vertical plates in the presence of 5 mM hydroxocobalamin. (I-L) Root hair phenotype of wild type, *cas-c1*, *rhd2-1* and *rhd2-1 cas-c1* 7-d-old plants, respectively, grown on MS pH4

sucrose vertical plates in the absence of 5 mM hydroxocobalamin. (M-P) Root hair phenotype of wild type, *cas-c1*, *rhd2-1* and *rhd2-1 cas-c1* 7-d-old plants, respectively, grown on MS pH4 in the presence of 5 mM hydroxocobalamin. All the experiments were repeated at least three times, with similar results obtained each time. Bars = 0.5 mm.

Figure 4. Root hair formation genes expression analysis. Real-time (RT)–PCR analysis of the expression of the *RHD6*, *RSL4, FLA6* and *MRH5* genes was performed in root extracts from 14-day-old wild-type, *cas-c1, scn1-1* and *scn1-1 cas-c1* mutants grown in MS pH 5,7 (A) or wild-type, *cas-c1, rhd2-1* and *rhd2-1 cas-c1* mutants grown in MS pH 4 (B). The transcript levels were normalized to the constitutive *UBQ10* gene. Data shown are means ± SD of three independent experiments. Different letters above the bar indicate significant different mean (ANOVA test, $P<0.01$).

Figure 5. Detection of superoxide in Arabidopsis roots. (A) Wild-type, (D) *cas-c1,* (B) *scn1-1,* (E) *scn1-1 cas-c1,* (C) *rhd2-1* and (F) *rhd2-1 cas-c1* seedlings were grown for 3 d on MS medium with sucrose. The roots were stained with NBT as described in Materials and Methods. Representative images are shown. All the experiments were repeated at least three times, with similar results obtained each time. Bars = 0.1 mm.

Figure 6. Accumulation of H_2O_2 in wild type and root hair mutants. H_2O_2 was detected by H_2DCFDA staining in 14-d-old roots of (A) wild-type, (D) *cas-c1,* (B) *scn1-1,* (E) *scn1-1 cas-c1*, (C) *rhd2-1* and (D) *rhd2-1 cas-c1* plants cultured on MS medium supplemented with 1% sucrose. All the experiments were repeated at least three times, with similar results obtained each time. Bars = 300 μm.

Figure 7. Involvement of CAS-C1 and cyanide in the root hair growth. In an elongating root hair, SCN1 inhibits the ROPs proteins, which are essential for the NADPH oxidase RHD2 tip-localized action. RHD2 produces superoxide anion (stained with NBT) that is transformed to oxygen peroxide (visualized by H_2DCFDA staining) by superoxide dismutase action. Both ROS are important for cell wall growth by breaking and rebuilding. Cyanide concentration, controlled by CAS-C1 and eliminated by COB, would act in a step between the SCN1 action and the ROS production by RHD2, establishing positive (arrows) or negative (blunt lines) relationships to hitherto unknown protein(s) or factor(s). Full lines indicate already established relationships, while dashed lines indicate the proposed sequence of action of CAS-C1 and cyanide in the root hair elongation process.

Supplementary Fig. S1. Schematic representation of the CAS-C1 locus and flanking genes on chromosome 3. A, Diagram of the intergenic sequence between *CAS-C1* and the adjacent genes on chromosome 3 of the Arabidopsis genome (www.arabidopsis.org). Yellow arrows indicate the direction of transcription of the different genes. Dark arrows indicate the designed oligonucleotide positions for *ProC1:CASC1* sequence isolation. B, The nucleotide sequence of *ProC1:CASC1*, where *ProC1* is the *CAS-C1* promoter, and *CASC1* is the *CAS-C1* ORF. Colored letters indicate intron (purple), UTR (red) and exon (yellow) sequence. Blue shadowed letters show the translational start and stop codons. *PIP-1* codes for a plasma membrane intrinsic protein and *SYP-73* codes for a syntaxin of plants.

Supplementary Fig. S2. Mitochondrial localization of CASC1-GFP (A) Maximum projection of 20 optical sections of 4-d-old root tissues from wild type plants transformed with *ProC1:CASC1-GFP* showing GFP fluorescence signal. (B) Fluorescence signal of the same tissues dyed with MitoTracker Deep Red 633 for 15 min, (C) Overlapping of (A) and (B) images showing co-localization of GFP fluorescence and stained mitochondria. Bars = 40 µm.

Supplementary Fig. S3. Root phenotype of the *cas-c1* and complemented mutant line. (A) Representative bright-field image of 4-day-old *cas-c1* mutant plants is shown. (B-C) Representative bright-field and GFP fluorescence images, respectively, of 4-day-old *cas-c1* mutant plants transformed with *ProC1:CASC1-GFP* are shown. Images are maximum projection of 20 optical sections. Bars = 50 µm

Supplementary Fig. S4. Molecular characterization of the *scn1-1 cas-c1* mutant. To identify individuals homozygous for *SCN1* and *CAS-C1* gene mutations, genomic DNA was extracted from leaves of wild-type and eight *scn1-1 cas-c1* mutants grown in MS medium supplemented with sucrose (1%) and kanamycin (30 µg/mL) and transplanted to soil later. This DNA was subjected to the following: A, PCR genotyping using the primer pairs scn1-1 FW/scn1-1 REV and C1-F2/C1-R2, with *UBQ10* amplification using UBQF1-UBQR1 as a positive control; B, sequencing genotyping using scn1-1 FW/scn1-1 REV primers.

scn1-1 FW: 5′-TCAAAGAACATCTCGAGAAGGA-3′

scn1-1 REV: 5′-CACACAAACACACCTCCAATGT-3′

C1-F2: 5′-TGATGGGAATTGGCAGTGGAGGCAC-3′

C1-R2: 5′-AATTGCTTGCCACGGTGTTAGCTCCC-3′

UBQF1: 5'- GATCTTTGCCGGAAAACAATTGGAGGATGGT-3'

UBQR1: 5'- CGACTTGTCATTAGAAAGAAAGAGATAACAGG-3'

Supplementary Fig. S5. Molecular characterization of the *rhd2-1 cas-c1* mutant. To identify individuals who were homozygous for *RHD2* and *CAS-C1* gene mutations, genomic DNA was extracted from leaves of wild-type, *rhd2-1* mutant (as positive control) and five *rhd2-1 cas-c1* mutants grown in MS medium supplemented with sucrose (1%) and kanamycin (30 µg/mL) and transplanted to soil later. This DNA was subjected to the following: A, PCR genotyping using the primer pairs rhd2-1 FW/rhd2-1 REV and C1-F2/C1-R2, with *UBQ10* amplification using UBQF1-UBQR1 was used as a positive control; B, sequencing genotyping using rhd2-1 FW/rhd2-1 REV primers.

rhd2-1 FW: 5´-TGAATGGTATGAACCAAACCGC-3´

rhd2-1 REV: 5´-GGCTTACACACCTGAAACAACA-3´

Supplementary Fig. S6. 1-Aminocyclopropane-1-carboxylic acid (ACC) effect on root hair formation. (A, C, E, G, I, K) Root hair phenotype of wild type, *cas-c1, scn1-1, scn1-1cas-c1, rhd2-1* and *rhd2-1 cas-c1* 6-d-old plants, respectively, grown on MS sucrose vertical plates in the absence of ACC. (B, D, F, H, J, L) Root hair phenotype of wild type, *cas-c1, scn1-1, scn1-1cas-c1, rhd2-1* and *rhd2-1 cas-c1* 6-d-old plants, respectively, grown on MS sucrose vertical plates in the presence of 50 µM ACC. Bars = 0.15 cm.

Supplementary Fig. S7. Cyanide determination in root tissues. Fourteen-days old wild type, *cas-c1, scn1-1, scn1-1 cas-c1, rhd2-1 and rhd2-1 cas-c1* mutant plants were grown on plates containing MS sucrose medium and then collected for cyanide content determination. Values are the means ± SD from five independent experiments. Increases of the media of the cyanide content in every couple of mutants are indicated at the top of the respective column pair. Asterisks indicate significant differences (ANOVA test, P<0,01) between wild type and *cas-c1* and between pairs of single and double mutants.

Supplementary Video S1. Root hair growth. *ProC1:CASC1-GFP* plants were grown for 2 d and fluorescence microscopy images were taken every 2 min over 2 h to analyze root hair formation *in vivo*. Bar = 25 µm.

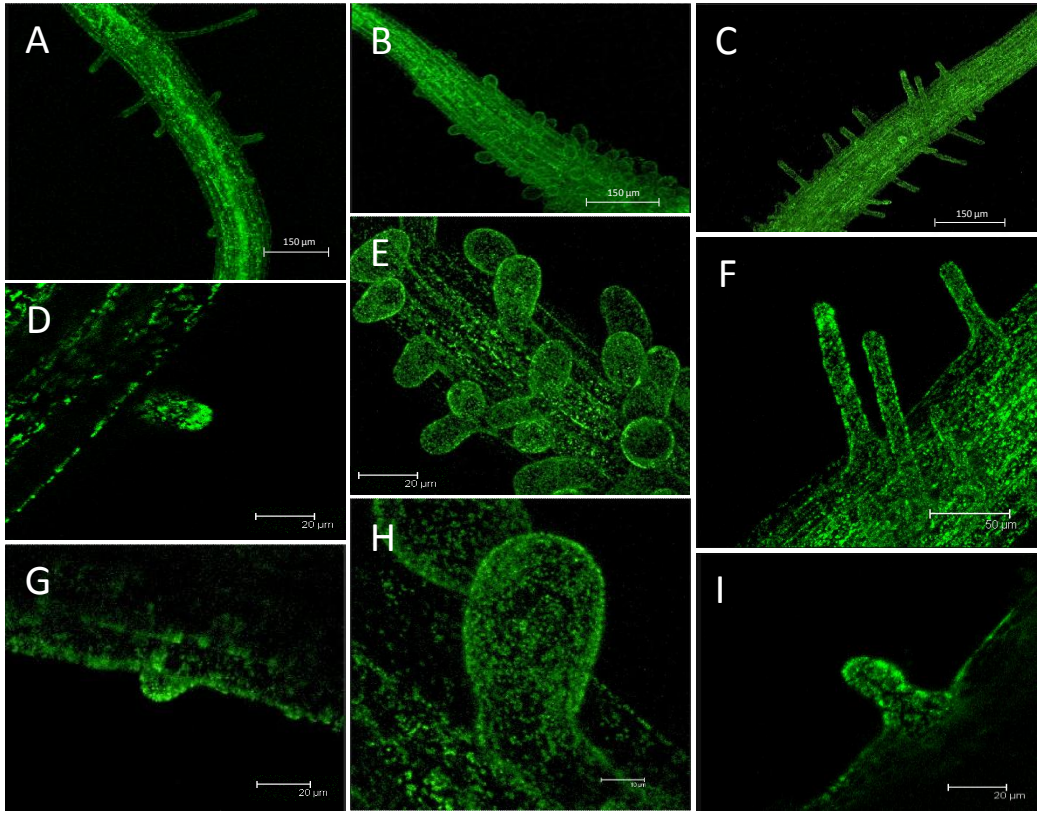

Fig. 1. CAS-C1 expression and localization study. Representative GFP images of A,D,G, wild type, B,E,H, *scn1-1* mutant and C,F,I, *rhd2GK* mutant transformed with *ProC1:CASC1-GFP*. Plants were grown in MS medium supplemented with sucrose for 2 days. Images are maximum projection of 20 optical sections.

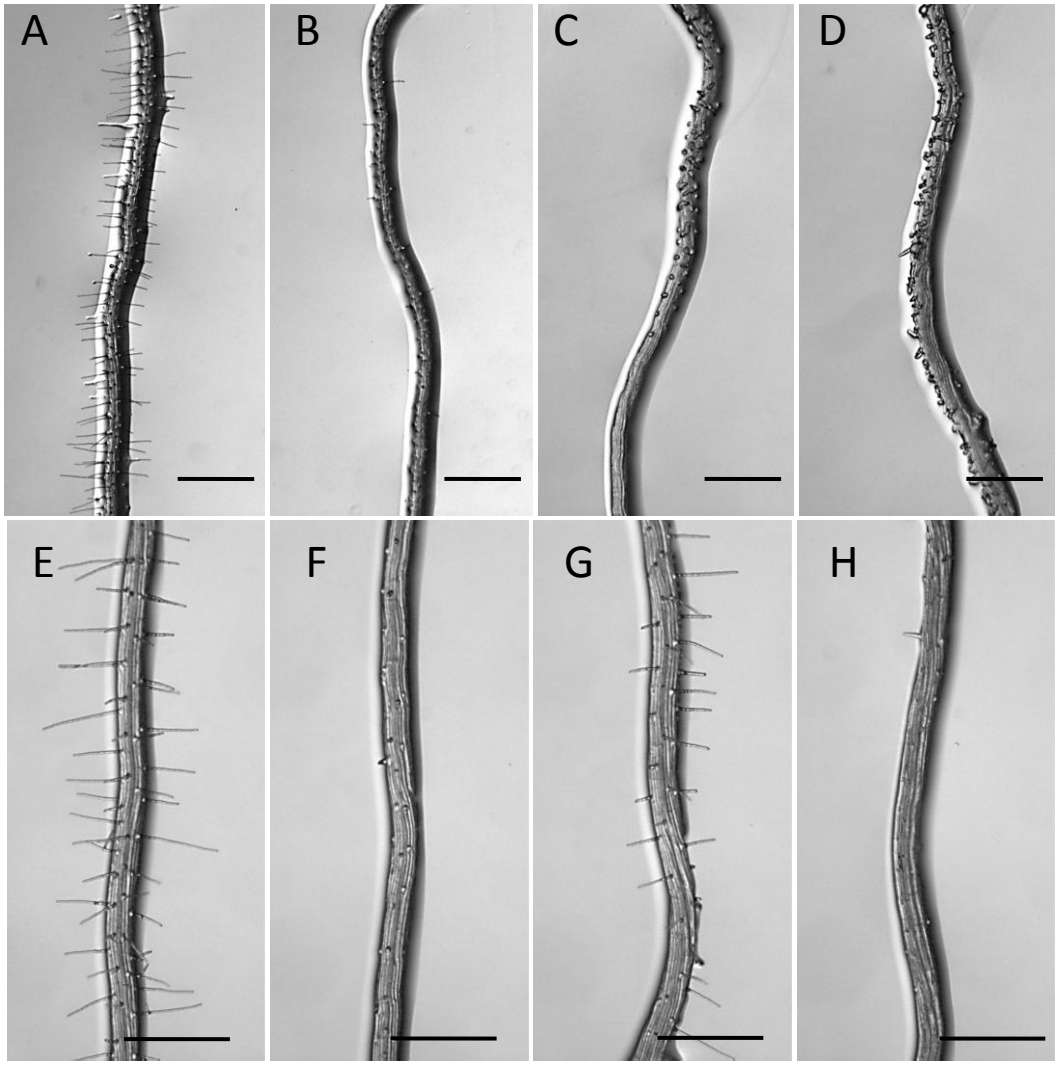

Fig. 2. Root hair phenotypes of root hair formation mutants. (A, E) Wild type, (B, F) *cas-c1*, (C) *scn1-1*, (D) *scn1-1 cas-c1*, (G) *rhd2-1, (*H) *rhd2-1 cas-c1* . Seedlings were grown 6-d on MS (A-D) or 7-d on MS pH4 (E-H) medium supplemented with sucrose in vertical plates. Representative images are shown. Bars = 0.5 mm.

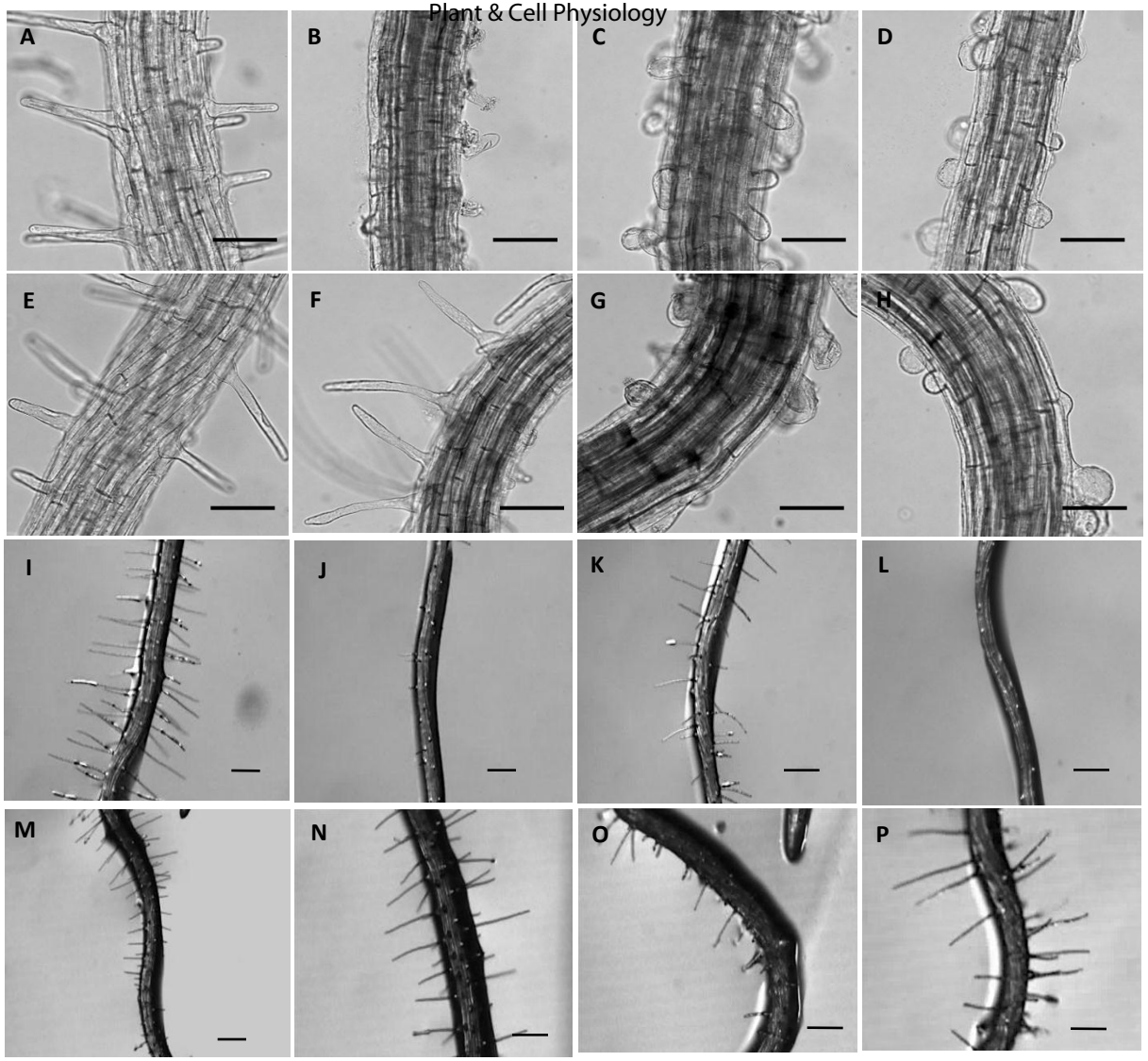

Fig. 3. Hydroxocobalamin effect on root hair formation. (A-D) Root hair phenotype of wild type, *cas-c1*, *scn1-1* and *scn1-1cas-c1* 3-d-old plants, respectively, grown on MS sucrose vertical plates in the absence of hydroxocobalamin. (E-H) Root hair phenotype of wild type, *cas-c1*, *scn1-1* and *scn1-1cas-c1* 3-d-old plants, respectively, grown on MS sucrose vertical plates in the presence of 5 mM hydroxocobalamin. (I-L) Root hair phenotype of wild type, *cas-c1*, *rhd2-1* and *rhd2-1 cas-c1* 7-d-old plants, respectively, grown on MS pH4 sucrose vertical plates in the absence of 5 mM hydroxocobalamin. (M-P) Root hair phenotype of wild type, *cas-c1, rhd2-1* and *rhd2-1cas-c1* 7-d-old plants, respectively, grown on MS pH4 in the presence of 5 mM hydroxocobalamin. All the experiments were repeated at least three times, with similar results obtained each time. Bars = 0.5 mm.

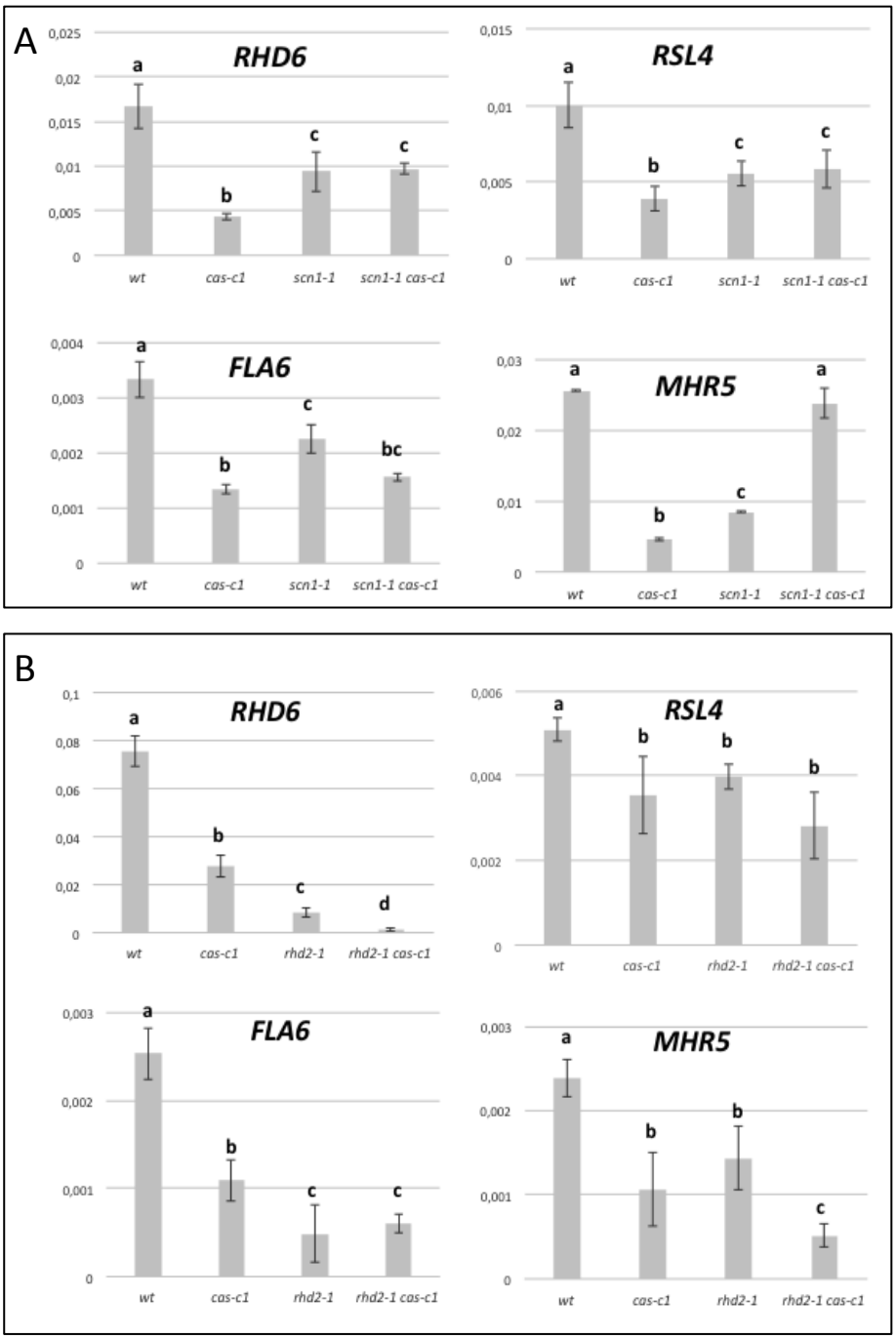

Fig. 4. Root hair formation genes expression analysis. Real-time (RT)–PCR analysis of the expression of the *RHD6*, *RSL4*, *FLA6* and *MRH5* genes was performed in root extracts from 14-day-old wild-type, *cas-c1*, *scn1-1* and *scn1-1 cas-c1* mutants cultured in MS pH 5,7 (A) or wild-type, *cas-c1*, *rhd2-1* and *rhd2-1 cas-c1* mutants cultured in MS pH 4 (B). The transcript levels were normalized to the constitutive *UBQ10* gene. Data shown are means ± SD of three independent experiments. Different letters above the bar indicate significant different mean (ANOVA test, P<0.01).

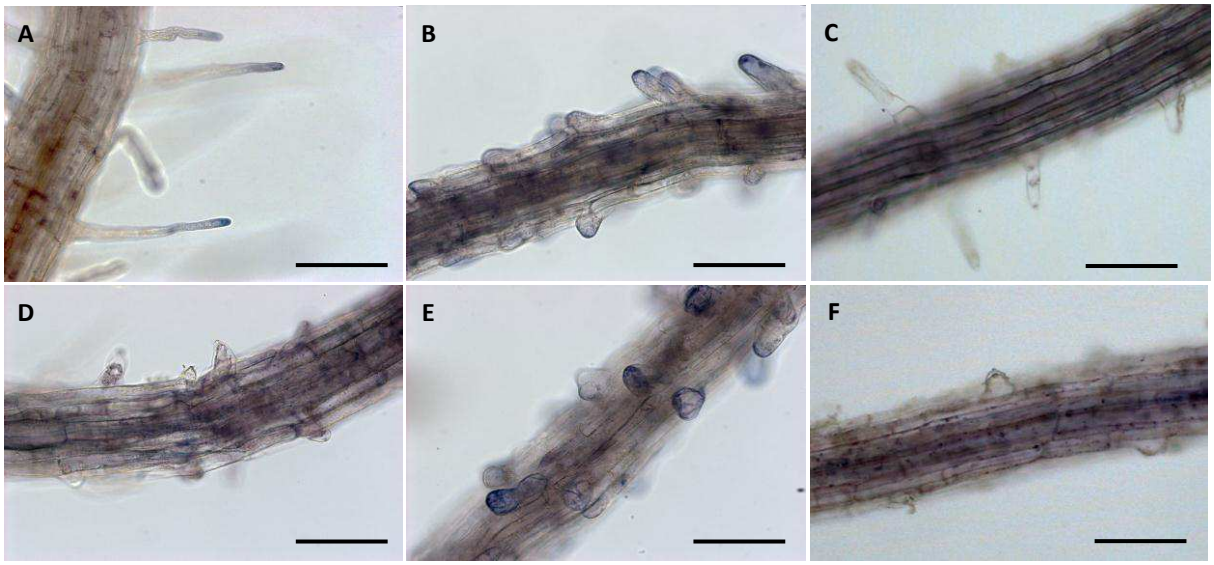

Fig. 5 Detection of superoxide in Arabidopsis roots. (A) Wild-type, (D) *cas-c1*, (B) *scn1-1*, (E) *scn1-1 cas-c1*, (C) *rhd2-1* and (F) *rhd2-1 cas-c1* seedlings were grown for 3 d on MS medium with sucrose. The roots were stained with NBT as described in Materials and Methods. Representative images are shown. All the experiments were repeated at least three times, with similar results obtained each time. Bars = 0.1 mm.

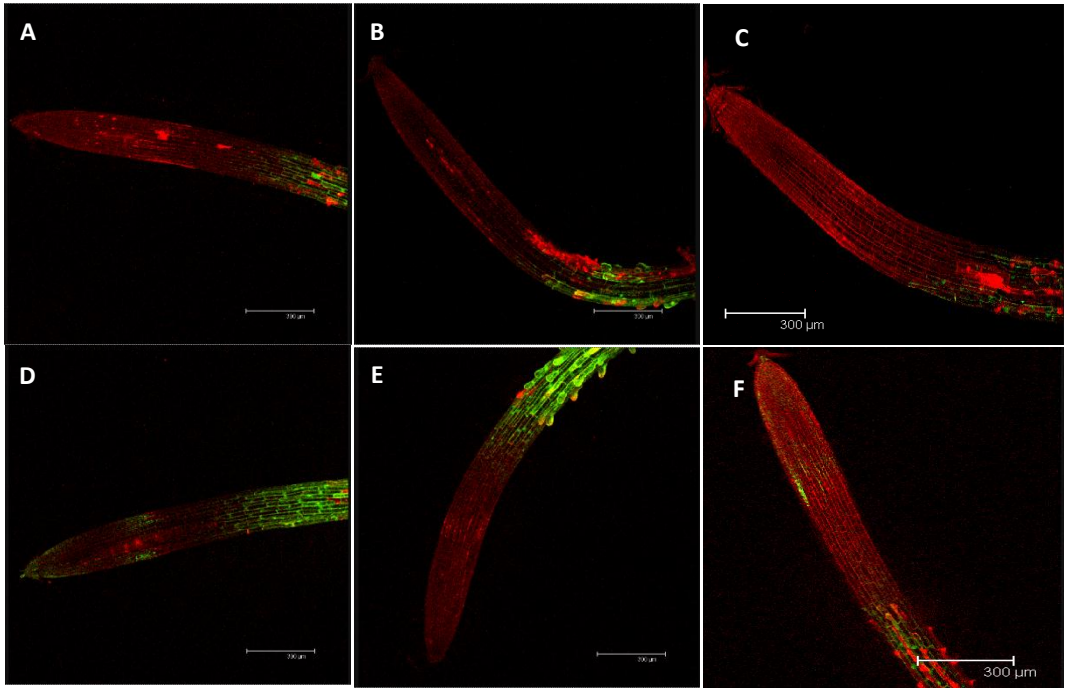

Fig. 6 Accumulation of H_2O_2 in the wild type and the root hair mutants. H_2O_2 was detected by H_2DCFDA staining in 14-d-old roots from (A) wild-type, (D) *cas-c1*, (B) *scn1-1*, (E) *scn1-1 cas-c1*, (C) *rhd2-1* and (F) *rhd2-1 cas-c1* mutants cultured in MS medium supplemented with sucrose. All the experiments were repeated at least three times, with similar results obtained each time. Bars = 300 µm.

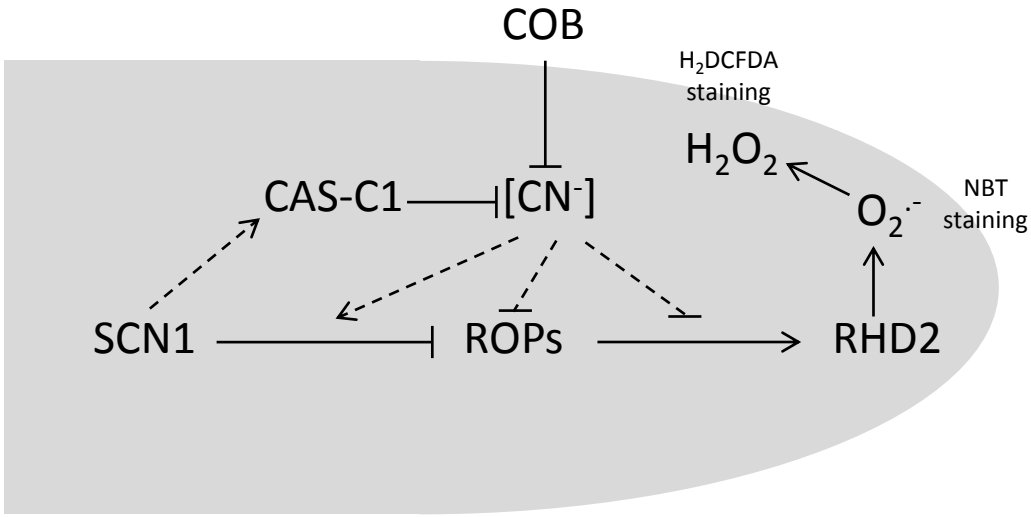

Fig. 7. Involvement of CAS-C1 and cyanide in the root hair growth. In an elongating root hair, SCN1 inhibits the ROPs proteins, which are essential for the NADPH oxidase RHD2 tip-localized action. RHD2 produces superoxide anion (stained with NBT) that is transformed to oxygen peroxide (visualized by H_2DCFDA staining) by superoxide dismutase action. Both ROS are important for cell wall growth by breaking and rebuilding. Cyanide concentration, controlled by CAS-C1 and eliminated by COB, would act in a step between the SCN1 action and the ROS production by RHD2, establishing positive (arrows) or negative (blunt lines) relationships to hitherto unknown protein(s) or factor(s). Full lines indicate already established relationships, while dashed lines indicate the proposed sequence of action of CAS-C1 and cyanide in the root hair elongation process.